

See discussions, stats, and author profiles for this publication at: <https://www.researchgate.net/publication/326204806>

Experimental evaluation and thermodynamic modelling of AILs alkyl chain elongation on methane riched gas hydrate system

Article in Fluid Phase Equilibria · July 2018

DOI: 10.1016/j.fluid.2018.07.003

CITATIONS

0

READS

17

4 authors, including:



Muhammad Saad Khan
Universiti Teknologi PETRONAS

25 PUBLICATIONS 53 CITATIONS

[SEE PROFILE](#)



Bhajan Lal
Universiti Teknologi PETRONAS

70 PUBLICATIONS 473 CITATIONS

[SEE PROFILE](#)

Some of the authors of this publication are also working on these related projects:



Gas hydrate mitigation through ammonium based ILs [View project](#)

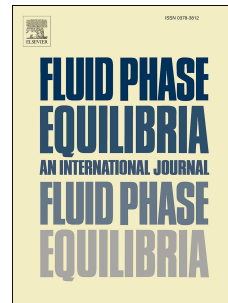


co2 capture [View project](#)

Accepted Manuscript

Experimental evaluation and thermodynamic modelling of AILs alkyl chain elongation on methane riched gas hydrate system

Muhammad Saad Khan, Bhajan Lal, Lau Kok Keong, Khalik Mohamad Sabil



PII: S0378-3812(18)30261-9

DOI: [10.1016/j.fluid.2018.07.003](https://doi.org/10.1016/j.fluid.2018.07.003)

Reference: FLUID 11880

To appear in: *Fluid Phase Equilibria*

Received Date: 3 March 2018

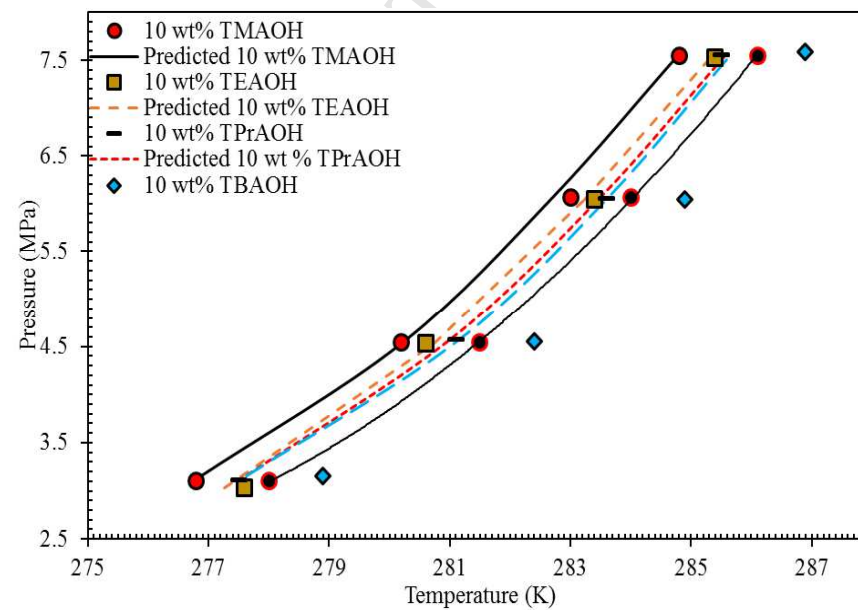
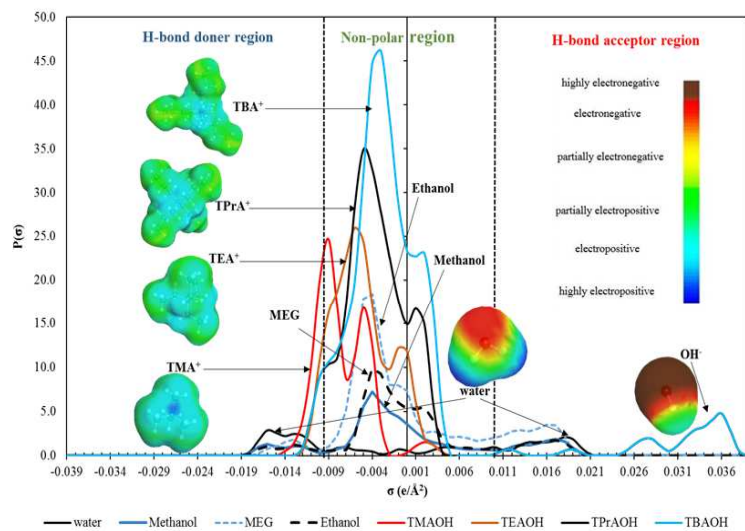
Revised Date: 21 June 2018

Accepted Date: 3 July 2018

Please cite this article as: M.S. Khan, B. Lal, L.K. Keong, K.M. Sabil, Experimental evaluation and thermodynamic modelling of AILs alkyl chain elongation on methane riched gas hydrate system, *Fluid Phase Equilibria* (2018), doi: 10.1016/j.fluid.2018.07.003.

This is a PDF file of an unedited manuscript that has been accepted for publication. As a service to our customers we are providing this early version of the manuscript. The manuscript will undergo copyediting, typesetting, and review of the resulting proof before it is published in its final form. Please note that during the production process errors may be discovered which could affect the content, and all legal disclaimers that apply to the journal pertain.

Graphical Abstract



1 **Experimental Evaluation and Thermodynamic Modelling of AILs**
2 **Alkyl Chain Elongation on Methane Riched Gas hydrate System**

3 Muhammad Saad Khan^{1,2}, *Bhajan Lal^{1,2}, Lau Kok Keong^{1,2} and Khalik Mohamad Sabil³

4

5 *Corresponding author: bhajan.lal@utp.edu.my

6 ¹CO₂ Research Centre (CO₂RES), Universiti Teknologi PETRONAS, Bandar Seri Iskandar, 32610,
7 Perak, Malaysia.

8 ²Chemical Engineering Department, Universiti Teknologi PETRONAS, Bandar Seri Iskandar, 32610,
9 Perak, Malaysia.

10 ³Institute of Petroleum Engineering, School of Energy, Geoscience, Infrastructure and Society, Heriot-
11 Watt University Malaysia, No 1 Jalan Venna P5/2, Precinct 5, 62200, Putrajaya, Federal Territory of
12 Putrajaya, Malaysia.

13 **Abstract**

14 In this study, the thermodynamic inhibition of CH₄ rich binary mixed hydrate system
15 (70-30 mole% CH₄ + CO₂) is reported for four ammonium based ionic liquids (AILs)
16 via experimental and modelling approaches. The T-cycle technique applied for the
17 characterization of the AILs namely tetramethylammonium hydroxide (TMAOH),
18 tetraethylammonium hydroxide (TEAOH), tetrapropyl ammonium hydroxide
19 (TPrAOH) and tetrabutylammonium hydroxide (TBAOH). The hydrate liquid-vapour
20 equilibrium (HL_wVE) conditions of studied systems measure within the temperature
21 and pressure ranges of 275.0-286.0 K and 3.0 – 7.50 MPa respectively at 10wt%
22 aqueous AILs solutions. All the studied AILs except TBAOH inflicted the THI
23 influence by shifting the HL_wVE of CH₄ enrich mixed gas hydrates. Elongation in
24 AILs alkyl chain length attributed to decrease the average hydrate suppression
25 temperature (ΔT). At 10 wt%, TMAOH exhibited the maximum inhibition impact
26 with a ΔT value of 1.28 K, followed by TEAOH (0.8 K), TPrAOH (0.7 K), and
27 TBAOH (-0.84 K) respectively. Instead of hydrate inhibitor, TBAOH worked as gas
28 hydrate promotor owing to the presence of relatively higher alkyl chain cation (butyl)
29 make it semi-clathrate hydrate. The study further extended for different
30 concentrations (1, 5 and 10 wt%) of TMAOH among the best considered AIL in this
31 study. COSMO-RS investigation is also incorporated to further understand the
32 thermodynamic inhibition behaviour of AILs via sigma profile analysis. Additionally,
33 the enthalpies of hydrate dissociation for all studied AILs systems also calculated via
34 Clausius-Clapeyron equation in this study. The calculated hydrate dissociation
35 enthalpies data revealed that all the studied AILs except TBAOH show insignificant
36 participation in mixed gas hydrate cage formation, therefore, do not form semi-
37 clathrate hydrates. However, enthalpy data of TBAOH revealed that it participated in
38 hydrate crystalline structure, therefore, worked as semi-clathrate hydrate.
39 Furthermore, the HL_wVE predictions of studied systems also performed via
40 electrolyte based model proposed by Dickens and Quinby-Hunt and found in
41 respectable agreement with the experimental data.

42 **Keywords**— Ammonium based Ionic Liquids (AILs); alkyl chain; CH₄ rich gas
43 hydrates; HL_wVE, ionic liquids; THI.

44 **INTRODUCTION**

45 Clathrate hydrate or gas hydrate are non-stoichiometric solid crystalline inclusion
46 compound formed due to the hydrogen-bonded water molecules as a host and small
47 size ($<10 \text{ \AA}$) gas as a guest molecule in thermodynamically favourable environments.
48 Commonly three hydrate structures; sI, sII and sH hydrate are found in nature. Small
49 guest gases like methane (CH_4) and carbon dioxide (CO_2) formed sI hydrates [1].

50 Formation of gas hydrates or clathrate hydrates is among the significant flow
51 assurance problems. Gas hydrates formation not solitary averts hydrocarbon
52 production it also obstructs in transportation and processing phases as well [2,3]. As
53 the gas and oil production moves to a more in-depth geographical location where
54 encountered added thermodynamically favourable conditions for hydrate formation,
55 the gas exploration is getting more prone to hydrate happenstances. Additionally, the
56 presence of small impurities, like CO_2 , hydrogen sulphide (H_2S) in the CH_4 system
57 leads to further hydrate happenstances. Since CO_2 more prone to hydrate formation;
58 the formation pressure of CO_2 is much lower than the uncontaminated CH_4 systems,
59 therefore, it significantly influenced on phase boundary of CH_4 gas [4].

60 Oil and gas industry paid enormous expenses; approximately USD 1 million
61 annually per mile for the insulation of off-shore pipelines and further hundreds of
62 million dollars spent on various conventional approaches [5–7]. To avoid gas hydrate
63 formations industry typically practices four common methods heating/insulation of the
64 pipeline, depressurization, removal of water together with chemical insertion. In most
65 of the cases, chemical inhibition is the only viable preventive method applied for gas
66 hydrate mitigation[8]. The chemical inhibitors further divided into thermodynamic
67 inhibitors (THIs) and low dosage hydrate inhibitors (LDHIs).

68 The THIs (methanol and mono-ethylene glycol (MEG)) applied in massive
69 compositions 10-50 wt% to form effective hydrogen bonding with water molecules
70 thus shifts the hydrate phase equilibrium curve towards lower temperature and higher
71 pressure regions to enhance hydrate free zone [9]. The problems related to
72 conventional THIs are their volatile nature together with the large quantities
73 requirements leads the more extensive storage facilities in the off-shore applications.
74 The LDHIs used in lesser quantities 0.50-2.0 wt% than THIs, and are divided into
75 kinetic hydrate inhibitors (KHIs) and Anti Agglomerates (AAs). KHIs typically based

76 on hydrophilic polymers (Polyvinylpyrrolidone (PVP) and polyvinylcaprolactam
77 (PVCap) which delays the nucleation and hydrate formation by intermingling at the
78 water-gas interface thus offers steric hindrance between the gas and water. On the
79 other hand, AAs belong to surfactants family; they do not prevent hydrate formation,
80 but they keep tiny hydrate particles into a form of hydrate slurry and are not allow
81 hydrates to agglomerate into large masses (hydrate plugs). The LDHs found less
82 effective in higher sub-cooling conditions which usually encounter in deeper-water
83 pipelines often attributed to the catastrophic hydrate growth [10].

84 Therefore, the quest for non-volatile, relatively environmentally friendly, innovative
85 and dual functional hydrate inhibitors leads researchers towards liquid salts, i.e. ionic
86 liquids (ILs). Xiao and Adidharma [11] initially used six imidazolium-based ILs
87 (IMILs) for dual functional gas hydrate inhibitors for CH₄ hydrate. They found that
88 studied ILs can shift hydrate equilibrium conditions towards lower temperature
89 together with delayed hydrate formation. Most of the studied ILs for hydrate inhibition
90 in the literature based on IMIL studies [12–19]. Limited researchers have found on the
91 influence of other ILs families [14,17,20–23] (mainly ammonium based ionic liquids
92 (AILs) [24–29]) for gas hydrate mitigation. Similarly, Keshavarz *et al.* [21] inductee
93 the research on AILs by application of tetraethylammonium chloride (TEACl) with
94 IMILs and found that TEACl provided better THI impact compare to IMILs on CH₄
95 hydrates.

96 Tariq *et al.* [30] employed five different families of AILs at lower quantities (1 and
97 5 wt %) as dual-functional gas hydrate inhibitors for CH₄ hydrates and found that all
98 AILs were able to induce THI influence at moderate temperature condition (3.0-7.0
99 MPa). However, at higher pressure, the inhibition influence appears to be reduced
100 drastically, and few of the studied AILs disclosed promotional effect as well [30]. In
101 our earlier work, TMAOH was reported as a suitable thermodynamic inhibitor for
102 both pure CH₄ and CO₂ hydrate systems. The inhibition impact, i.e., average
103 suppression temperature (ΔT) of TMAOH was reported as 1.53 and 2.27 K for CH₄
104 and CO₂ hydrates respectively. Recently our lab also reported TMACl, TEAOH and
105 TPrAOH inhibitions up to 1.7 K, 1.6 K and 1.2 K respectively for CO₂ hydrates [4].
106 Table 1 represents the ΔT values of various systems for quantitative comparisons
107 purpose.

108 Table 1: Average suppression temperature (ΔT) of 10 wt% considered AILs samples
 109 for different systems and comparisons with literature data.

Studied System	T (K)		
	CH ₄	CO ₂	70-30 CH ₄ +CO ₂
	hydrate	hydrate	hydrate
TMAOH	1.53 [29]	2.27 [29]	1.28 (this study)
TEAOH	-	1.67 [4]	0.78 (this study)
TPrAOH	-	1.22 [4]	0.70 (this study)
TBAOH	-	-	-0.84 (this study)
Glycine [31,32]	1.78	1.83	-
Alanine [31,32]	1.55	1.68	-
Proline [31,32]	1.43	1.44	-
Serine [31,32]	1.29	1.21	-
Arginine [31,32]	0.74	1.03	-
[OH-EMIM][Cl] [33]	1.70	-	-
Triethylene Glycol [34]	1.28	-	-
Mono Ethylene Glycol [35]	2.59	-	-
Mono Ethylene Glycol (CSMGem)	2.49	2.61	2.51
Methanol [35]	4.70	-	-
Methanol [36]	-	6.05	-
Glycerol [37]	-	1.66	-
[EMPip][BF ₄][38]	-	1.13	-
[EMPip][Br] [38]	-	1.27	-
[EMMor][Br] [38]	-	1.29	-
[EMMor][BF ₄] [38]	-	1.13	-
[BEPyrr][BF ₄][39]	-	0.75	-

110 Most of the ILs studies encompasses pure gas hydrates for CH₄ and CO₂ hydrates;
 111 however, insufficient literature available for mixed gas hydrate systems in the open
 112 literature. Ullah *et al.* [40] recently applied low concentrations (1 and 5 wt.%) of
 113 Choline-Chloride as THI for Qatari natural gas mixture and reported that 5 wt% of
 114 Choline-Chloride reduce ΔT up to 1.56 K. Nevertheless, 1 wt% displayed minor
 115 inhibition (ΔT) up to 0.5 K. Additionally, Qureshi *et al.* [41] worked with
 116 pyrrolidinium-based ILs (1-Methyl-1-Propylpyrrolidinium Triflate [PMPy][Triflate])

117 and Propylpyrrolidinium Chloride [PMPy][Cl]) for Quantary mixture of Qatar natural
118 gas for dual functional hydrate inhibitors. Their outcomes revealed that both ILs
119 displayed dual functional impact, at 5wt%, PMPy-Cl the phase boundary shift up to 1
120 K. Similarly, it can also slightly improve the induction time compare to pure water
121 [41]. Overall, an insufficient number of publications available for ILs with the mixed
122 gas system and none of the preceding studies were emphasized the impact of AILs on
123 CH₄ riched mixed gas hydrates.

124 Previously COSMO-RS software was used to determine the intermolecular
125 interactions of ILs-water system in hydrate system [42,43]. Preceding studies
126 suggested that in COSMO-RS, the sigma profile and hydrogen bonding are the two
127 standout properties that justified the THI inhibition performance of ILs and other
128 electrolytes [29,31,42,44]. Bavoh and co-workers [42] initially established that the
129 sigma profile can determine the miscibility behaviour and hydrogen bonding ability of
130 the ILs with water molecule which are the most fundamental properties pre-requisites
131 for THI behaviour.

132 Various modelling approaches in the presence of ILs had reported earlier in the
133 literature [19,39,45–49]. The THI behaviour induced due activity of chemical in the
134 aqueous phase. Therefore activity coefficient approach is mainly applied. Most of the
135 prior modelling studies only dealt with the pure gases systems like CH₄ and CO₂.
136 Likewise, the modelling studies of mixed gas systems in the presence of ILs are scarily
137 intermittent. Recently, our group applied the electrolyte based Dickens and Quinby-
138 Hunt [50] model for CO₂ riched system [51]. Henceforth additional experimental and
139 modelling investigations of ILs especially AILs on differently mixed gas hydrate
140 systems are essential to discover the impact of AILs on phase behaviour.

141 Therefore, this work covers the THI performance of four AILs on CH₄ rich binary
142 mixed gas hydrates system (70-30 mole% CH₄ + CO₂). The selection of AILs
143 encompasses the elongation of the alkyl chain length on the inhibition performance.
144 The thermodynamic inhibition impact of AILs + CH₄+ CO₂ for 70-30 mole % systems
145 are measured at a temperature and pressure ranges of 276-286 K and 3.0-7.50 MPa
146 respectively. COSMO-RS software is used to analyze AILs- water system interactions
147 via Sigma profile graph for better understanding the inhibition mechanisms. Besides,
148 the Clausius–Clapeyron equation also applied for calculating the hydrate dissociation

149 enthalpy of each considered system. Additionally, the electrolyte model proposed by
 150 Dickens and Quinby-Hunt [50] used for predicting Hydrate Liquid-Vapor Equilibrium
 151 (HL_w VE) data of a considered system in the presence of aqueous AILs solutions.

152 **METHODOLOGY**

153 **Materials**

154 The details of chemicals use in this study are layout in Table 2. All the studies
 155 chemicals are purchased from Merck milli-pore Germany and applied without any
 156 further purification. The mixed gas purchased from Gas Walker Sdn. Bhd., Malaysia.
 157 Deionized water was used to prepare desired concentrations of AILs in all samples.
 158 For accurate weight measurements of the samples, HR-250AZ analytical balance was
 159 used with an accuracy of ± 0.3 mg.

160 **Table 2:** Details of chemicals employed in this work

S.No	Name of Chemical	Formula	Purity
1	water	H ₂ O	Deionized
2	Mixed Gas 70.001-29.999 mole% (CH ₄ + CO ₂)	G	70-30 mol % (Mixed gas)
3	Tetramethyl ammonium Hydroxide	TMAOH	25.0 wt% TMAOH, 75.0 wt% H ₂ O (Aqueous solution)
4	Tetraethyl ammonium Hydroxide	TEAOH	40.0 wt% TEAOH, 60.0 wt% H ₂ O (Aqueous solution)
5	Tetrapropyl ammonium Hydroxide	TPrAOH	40.0 wt% TEAOH, 60.0 wt% H ₂ O (Aqueous solution)
6	Tetrabutyl ammonium Hydroxide	TBAOH	40.0 wt% TEAOH, 60.0 wt% H ₂ O (Aqueous solution)

161 **Experimental details and procedure**

162 The high-pressure equilibrium cell with a volumetric capacity of 650 cm³ used in
 163 this study. The apparatus can operate within the ranges of 253–323 K and up to 20
 164 MPa. The reactor is equipped with the pressure transducer (GP-M250) and temperature
 165 sensor (Pt-100) to measure and record the pressure and temperature, respectively.
 166 These sensor devices efficiently work with an uncertainty of ± 0.01 MPa and ± 0.1 K,
 167 individually. Moreover, for providing adequate agitation, the mixture in the reactor is
 168 stirred by the magnetic stirrer at 400 rpm. An isochoric pressure search

169 Thermodynamic Cycle (T-cycle) technique is adopted to detect the HL_w VE data as
 170 applied in earlier studies [32,52] especially with mixed gas hydrate systems [53,54].
 171 Further details about the apparatus and detailed experimental procedure can found
 172 elsewhere [4,24,29,53].

173 *HL_w VE data analysis*

174 In this study average suppression temperature (ΔF) is calculated for the
 175 determination of inhibition influence of AILs on binary gas hydrate. ΔF has
 176 calculated via similar equation used in earlier work [11,52,55].

$$\Delta F = \frac{\sum \Delta T}{n} = \frac{\sum_{i=1}^n (T_{0,p_i} - T_{1,p_i})}{n} \quad (1)$$

177 where, T_0 , p_i denotes the equilibrium temperature of the mixed gas in a pure water
 178 sample (absence of AILs), while T_1 , p_i is the equilibrium temperature of the mixed gas
 179 in the presence of aqueous AILs solutions. The values of both dissociation
 180 temperatures attained at the same p_i and n denotes to the number of pressure point
 181 considered in the experiments.

182 *Dissociation Enthalpy (ΔH_{diss}) for mixed gas hydrate*

183 Determination of hydrate dissociation enthalpy (ΔH_{diss}) is critical for understanding
 184 the hydrate structure and guest cage occupancy, which directly associated with the
 185 size of the guest molecule and size of the cavity. The ΔH_{diss} in this work is estimated
 186 by the Clausius-Clapeyron equation as proposed by various researchers [4,13,56–59].

$$\frac{d \ln P}{d \frac{1}{T}} = \frac{\Delta H_{diss}}{zR} \quad (2)$$

187 Where ΔH_{diss} , T , P , R , z , are hydrate dissociation enthalpy, temperature, pressure,
 188 universal gas constant and compressibility factor respectively. The value of z is
 189 calculated by using the Peng-Robinson equation of state [19,60,61] for studied mixed
 190 gas system.

191 *COSMO-RS analysis of AILs-water system*

192 Molecular interaction through sigma profiles of AILs and water molecules are
 193 generated in COSMO-RS software to understand the detail THI inhibition
 194 mechanism. The COSMO-RS predictions are performed using COSMOthermX,
 195 Version C2.1 software. The sigma profiles generated by selecting water and AILs

196 molecules in the compound list with the parameter file BP_TZVP_C21_0111.ctd
 197 (COSMOlogic GmbH & Co KG, Leverkusen, Germany) via the lowest energy
 198 conformer [42,62–66].

$$ps(\sigma) = \frac{\sum_i x_i p^{xi(\sigma)}}{\sum_i x_i} \quad (3)$$

199 The distribution of the division given on the sigma (σ) is called σ -profile ($ps(\sigma)$).
 200 The σ -profile of the solvent $ps(\sigma)$, defined as the mole fraction (x_i) weighted sum of
 201 the σ -profiles of its compounds x_i , p^{xi} respectively in Equation 3.

202 *Thermodynamic model theory*

203 To predict the hydrate phase behaviour (HL_w VE) of the studied systems, the effect
 204 of additives (AILs) needs to be estimated for accurate determination of activity
 205 coefficient. Since AILs are salts in the liquid phase, therefore, the electrolyte based
 206 model proposed by Dickens and Quinby-Hunt [50] is employed in this work. The
 207 selected model is the amended version of the Pieroen [67] model and prior applied for
 208 several electrolytes studies like Amino acids [31,52] besides other ILs by Partoon *et*
 209 *al.* [48] and Javanmardi *et al.* [68,69].

210 The model principally established from the traditional thermodynamic conception
 211 which assumes that the amount of gas in the aqueous phase is trivial, and vice versa.
 212 In the same way, the impact of AILs on the mixed gas hydrate phase boundary is
 213 solitary to decrease the activity of water (a_w), and at minor temperature ranges, the
 214 hydrate enthalpy of dissociation (ΔH_{diss}) is constant. The brief derivation details have
 215 provided by Dickens and Quinby-Hunt [50] and Pieroen [67]. Based on this model,
 216 the outcome of AILs on the gas hydrate dissociation temperature can denote as;

$$\ln a_w = \frac{\Delta H_{diss}}{nR} \left[\frac{1}{T_w} - \frac{1}{T_{AILs}} \right] \quad (4)$$

$$\ln a_w = \frac{\Delta H_{FUS(i)}}{R} \left[\frac{1}{T_{f(i)}} - \frac{1}{T_f} \right] \quad (5)$$

217 Where a_w denoted water activity, n reflected the gas hydrate hydration number
 218 which taken as 5.75 due to methane-dominated gas system [19,52]. ΔH_{diss} represents
 219 the hydrate dissociation enthalpies of mixed gas hydrate (60.846 kJ/mol) obtained via
 220 CSMGem software, R is the universal gas constant, and T_w and T_{AILs} are the hydrate

221 formation temperatures in pure water and AILs solutions. $\Delta H_{FUS(i)}$ denoted as the heat
 222 of fusion of ice (6.008 KJ/mol), $T_{f(i)}$ and T_f are the freezing point temperatures of
 223 water (273.15 K) and water + AILs solutions. Freezing points of AILs (T_f) have
 224 calculated as proposed by Dickens and Quinby-Hunt [50] by using a cryoscopic
 225 constant of water as 1.853 K·kg/mol. Hereafter, merging the Eq. (4) moreover, (5),
 226 describes the temperature offset of methane hydrate phase condition and the
 227 temperature of the ice-water equilibrium condition in AILs solutions at constant
 228 pressure as follows;

$$\left[\frac{1}{T_w} - \frac{1}{T_{AILs}} \right] = \frac{n\Delta H_{FUS(i)}}{\Delta H_{diss}} \left[\frac{1}{T_{f(i)}} - \frac{1}{T_f} \right] \quad (6)$$

229 Therefore, Eq. (6) is applied to predict the hydrate dissociation temperature T_{AILs} ,
 230 in the presence of aqueous AILs solutions. For the reliability of the model predictions;
 231 average absolute deviation (AAE) is also calculated by using Eq. (7).

$$AAE = \frac{1}{n} \sum_{i=1}^n |T_{Exp.} - T_{Cal.}| \quad (7)$$

232 RESULTS AND DISCUSSION

233 *Influence of AILs on HL_w VE conditions of CH_4 riched mixed hydrate*

234 The HL_w VE for of G + H₂O and G + H₂O + AILs in the presence of 10wt% aqueous
 235 AILs are reported in Table 3. To assess the impact of alkyl chain elongation on the
 236 THI; studied AILs are evaluated at moderate pressure ranges (3.0-7.50 MPa), and
 237 hydrate equilibrium curves of G + H₂O + AILs are attained in the presence and
 238 absence of various aqueous AILs solutions at 10 wt% concentrations.

239

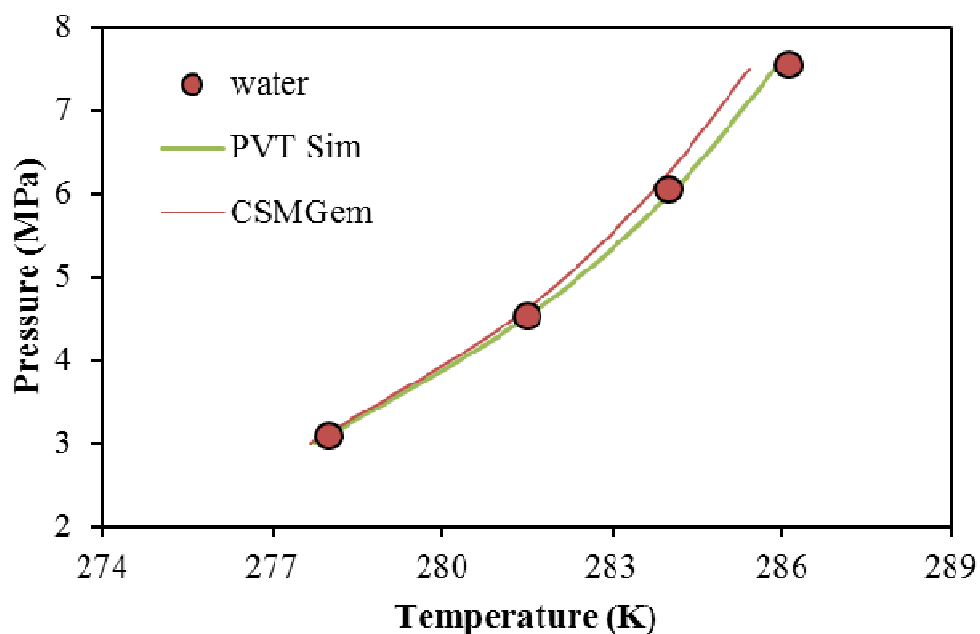
240 **Table 3:** The HL_w VE points of CH_4 rich mixed gas in the absence and the presence
 241 10 wt% AILs

AILs	Temperature (K)	Pressure (MPa)
Pure water	278.0	3.10
	281.5	4.54
	284.0	6.06
	286.1	7.55
TMAOH	276.8	3.04

	280.2	4.57
	283.0	6.10
	284.8	7.55
	277.6	3.03
TEAOH	280.6	4.53
	283.4	6.05
	285.4	7.53
	277.5	3.1
TPrAOH	281.1	4.56
	283.6	6.05
	285.5	7.55
	278.9	3.15
TBAOH	282.4	4.55
	284.9	6.05
	286.9	7.59

242 Expanded uncertainties $U(T) = \pm 0.1$ K; $U(P) = \pm 0.01$ MPa (0.95 level of confidence).

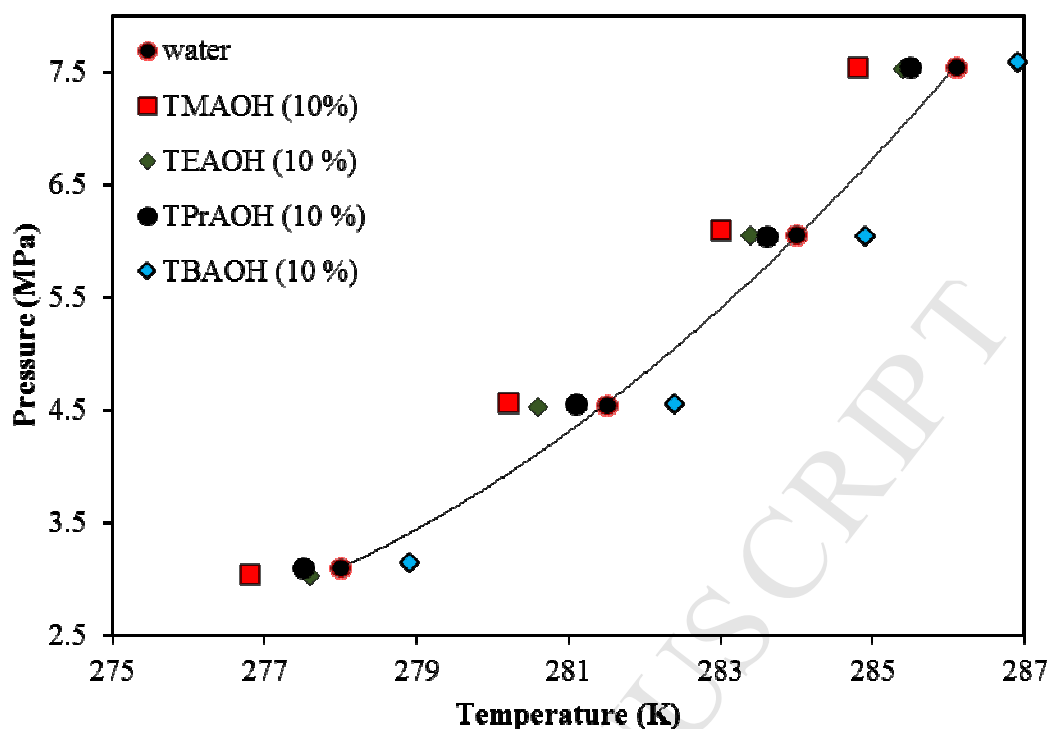
243 The HL_w VE data of the studied binary system is depicted in Figure 1. The HL_w VE
 244 phase boundary of studied hydrate system is further compared with the commercial
 245 hydrate prediction software CSMGem and PVTsim respectively. The studied mixed
 246 gas data (see Figure 1) was found in fair agreement with the HL_w VE prediction
 247 software (CSMGem and PVTsim) data.



248

249 **Figure 1:** HL_wVE data points of CH₄ riched mixed gas (G= 70-30 CH₄ + CO₂)
 250 G+H₂O hydrates in comparisons with commercial hydrate prediction soft wares
 251 (CSMGem and PVTsim).

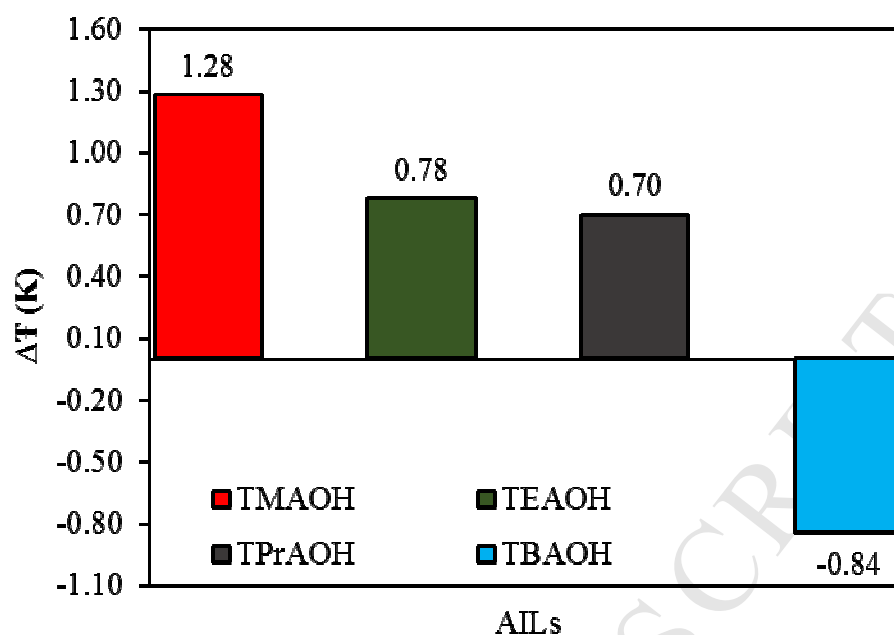
252 To evaluate the impact of alkyl chain elongation on THI performance; Figure 2
 253 illustrates the HL_wVE data of AILs + G + H₂O hydrates at 10 wt% concentration. The
 254 results revealed that with an increase (elongation) in alkyl chain length of studied
 255 AILs, the inhibition impact appears to be significantly reduced for the studied
 256 systems. The TMAOH performed best among the considered AILs and induced
 257 maximum inhibition via shifting the HL_wVE curves towards lower temperature and
 258 higher pressure regions (see Figure 2). TEAOH and TPrAOH are also able to shift the
 259 hydrate phase equilibrium towards higher pressure and lower temperature regions for
 260 studied concentration. On the contrary, at 10 wt% TBAOH did not act as a THI in its
 261 place shifts the HL_wVE curve towards lower pressure and higher temperature regions
 262 which considerably enhance the hydrate metastable region and ultimately functioned
 263 as gas hydrate promoter. The promotion behaviour of TBAOH has observed due to
 264 the possible formation of semi-clathrate structure owing to the TBA⁺ cation which
 265 has a tendency to be trapped in the hydrate cages as a non-gaseous guest at milder
 266 conditions which further discussed in later section [70,71].



267

268 **Figure 2:** The HL_w/VE phase behaviour of CH₄ rich mixed gas hydrates at 10 wt%
 269 AILs solutions.

270 To compare the quantitative impact of AILs on THI performance; the average
 271 depression temperature (ΔT) also reported for 10 wt% AILs solutions in Figure 3. The
 272 THI influence of AILs found in the following increasing magnitude: TBAOH <
 273 TPrAOH < TEAOH < TMAOH. Owing to the presence of the shortest alkyl chain
 274 TMAOH can deliver maximum inhibition ($\Delta T=1.28$ K) among the considered AILs.
 275 On the contrary, TBAOH ($\Delta T=-0.84$ K) reveal promotional result attributable to its
 276 potential semi-clathrate behaviour due to relatively elongated alkyl chain as stated in
 277 the previous studies [26,70,71].



278

279 **Figure 3:** Average suppression temperature (ΔT) of CH₄ mixed gas hydrates for 10
280 wt% aqueous AILs solutions.

281 The potential reasons for higher inhibition impact are concealed in the structure of
282 TMAOH. TMAOH retains TMA⁺ cation (shortest among the studied AILs) which
283 merely comprises one alkyl group (methyl) in their structure together with hydroxyl
284 (OH⁻) anion which offers adequate linkage on the surface of and water gas interface.
285 OH⁻ anion is already established as among the best anions that induce more hydrogen
286 bonding with water [4,14,42] owing to their smaller nuclei size (value of 0.169 nm)
287 which is relatively lower than all other halide anion except fluoride (F⁻ = 0.133
288 nm)[72,73]. Due to these reasons, TMAOH offer more hydrophilic behaviour
289 compared to other studied AILs (TBAOH, TPrAOH and TEAOH) resulted in more
290 THI inhibition [4,14,24].

291 To evaluate the impact of experimental pressure on the inhibition performance of
292 AILs Table 4 presents the hydrate suppression temperature of 10 wt% aqueous AILs
293 solutions at different experimental pressures. Results from Table 4 showed that at a
294 studied concentration (10 wt%) of aqueous AILs solutions the inhibition performance
295 is dependent on pressure variations (i.e., ΔT changes with experimental pressure
296 conditions for all AILs). This is evident due to the presence of the higher amount of
297 CH₄ in the studied mixed gas system [29]. Tariq et al. [30] also reported the similar
298 behaviour, as their studied AILs provide higher inhibition performance at moderate
299 pressure conditions (>6 MPa) beyond that pressure the inhibition performance
300 significantly reduced and some of them even worked as gas hydrate promoters.

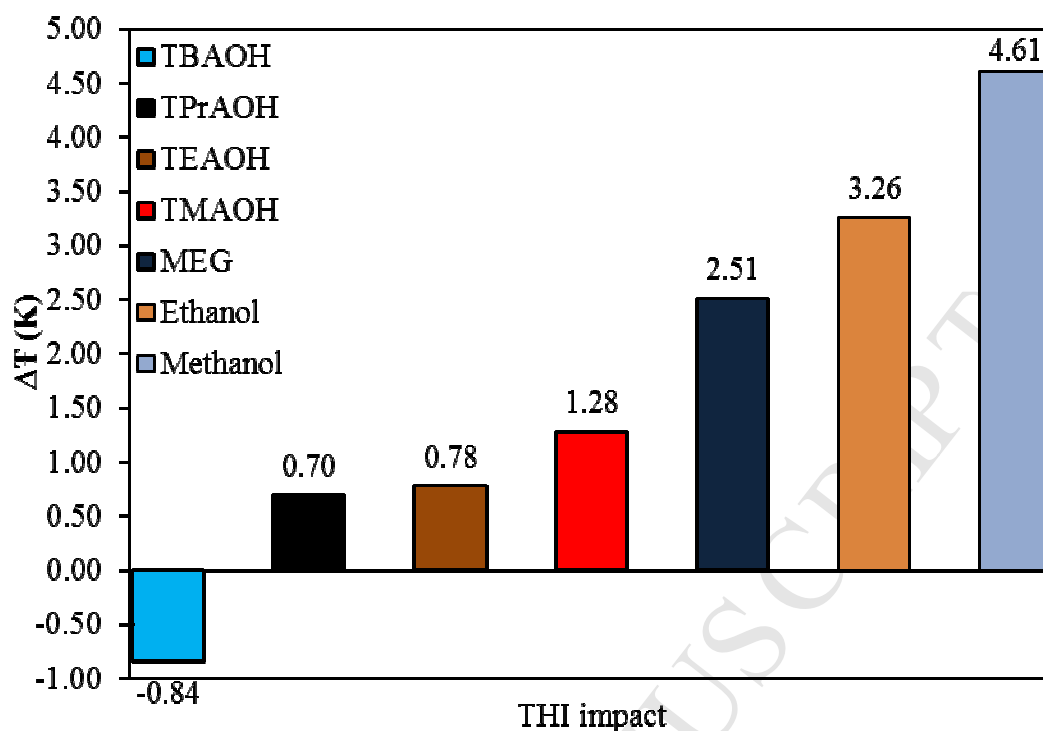
301 Additionally, in our earlier work [29], we observed that the inhibition performance of
 302 TMAOH also observed similar behaviour (ΔT varies with experimental pressures) for
 303 pure CH_4 hydrates, however in case of pure CO_2 hydrates there was no variation
 304 observed. Therefore, ΔT values are independent of experimental pressures.

305 **Table 4:** Suppression Temperature (ΔT) of mixed gas hydrate at different
 306 experimental pressures in the presence of 10 wt% aqueous AILs solutions

Pressure	TMAOH (10%)	TEAOH (10 %)	TPrAOH (10 %)	TBAOH (10 %)
P (MPa)	T (K)	T (K)	T (K)	T (K)
3.0	0.46	0.05	0.05	-0.81
4.50	1.51	1.05	1.02	-0.77
6.0	1.40	0.90	0.82	-1.03
7.50	0.92	0.37	0.25	-0.73
ΔT (K)	1.28	0.78	0.70	-0.84

307 Expanded uncertainties $U(T) = \pm 0.1 \text{ K}$ (0.95 level of confidence).

308 The acquired THI data of studied AILs are also compared with different commercial
 309 inhibitors, i.e., Methanol, Mono Ethylene Glycol (MEG) and Ethanol in Figure 4. The
 310 HL_w VE data of commercial inhibitors are generated via CSMGem. The obtained
 311 results exposed that commercial inhibitors accomplished superior THI impact
 312 compared to the considered AILs (see Figure 4), therefore suggesting that the more
 313 research on new combinations of ILs especially AILs are indispensable.



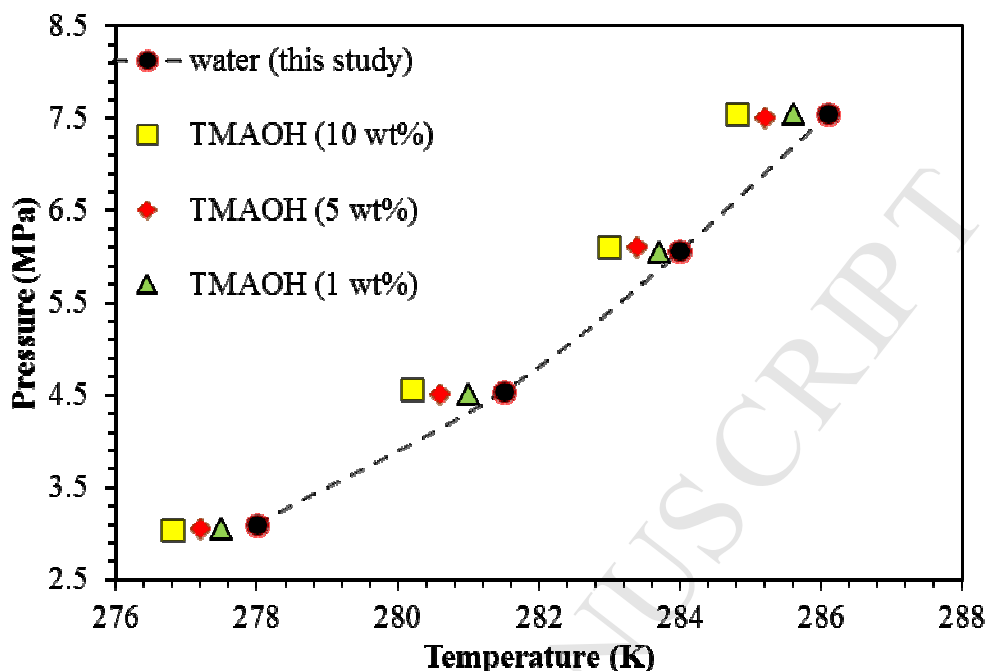
314

315 Figure 4: Comparison of THI impact (ΔT) of 10 wt% studied AILs with (CSMGem
316 software predicted) commercial inhibitors data.

317 As it observed from the Figure 3, TMAOH displays the better inhibition among the
318 considered AILs for CH_4 riched mixed gas hydrate systems. Therefore, the influence
319 of different TMAOH concentrations (1, 5 and 10 wt%) further investigated, and
320 tabulated in Table 5 and depicted in Figure 5.

321 **Table 5:** HL_w VE data of mixed gas hydrate in the presence of 1, 5 and 10 wt%
322 concentrations of aqueous TMAOH solutions

System	TMAOH Concentration							
	0 wt%		10 wt%		5 wt%		1 wt%	
	<i>T</i> (K)	<i>P</i> (MPa)	<i>T</i> (K)	<i>P</i> (MPa)	<i>T</i> (K)	<i>P</i> (MPa)	<i>T</i> (K)	<i>P</i> (MPa)
G + H₂O	278.0	3.10	276.8	3.04	277.2	3.05	277.5	3.05
+TMAOH	281.5	4.54	280.2	4.57	280.6	4.51	281.0	4.51
	284.0	6.06	283.0	6.10	283.4	6.10	283.7	6.05
	286.1	7.55	284.8	7.55	285.2	7.51	285.6	7.55



323

324 **Figure 5:** HL_w/VE phase boundaries of CH₄ rich mixed gas in the presence of the
325 various aqueous TMAOH concentrations.

326 Moreover, Table 6 reflects the suppression temperature (ΔT) of different
327 concentration of the TMAOH at various experimental pressures for mixed gas
328 hydrates. Results reveal that the inhibition impact of TMAOH is pressure and
329 concentration dependent. The ΔT value of 10 wt% (1.28 K) concentration stretch
330 more inhibition compares to lower concentrations of 5 (0.72 K) and 1 wt% (0.39 K).
331 It is also noticeable that the inhibition impact also varies with the experimental
332 pressures for each studied system (1, 5 and 10 wt %) of TMAOH. The higher
333 inhibition (ΔT) found at moderate pressure ranges (4.50 and 6.0 MPa) perhaps due to
334 the presence of CH₄ in the mixed gas. Subsequently, previous AIL-CH₄ studies also
335 stated the similar behaviour for methane hydrates [29,30] as mentioned above. For
336 further investigations, COSMO-RS study is also incorporated in next section to
337 further investigate the alkyl chain elongation of AILs by molecular interaction with
338 water.

339 **Table 6:** Suppression Temperature (ΔT) of CH₄ rich mixed gas hydrate in the
340 presence of different concentrations (1, 5 and 10 wt %) of TMAOH solutions.

TMAOH concentrations

Pressure (MPa)	10 wt%	5 wt%	1 wt%
3.0	0.46	0.29	0.05
4.50	1.51	1.22	0.87
6.0	1.40	0.98	0.63
7.50	0.92	0.37	0.02
ΔT (K)	1.28	0.72	0.39

341 Expanded uncertainties $U(T) = \pm 0.1$ K, (0.95 level of confidence).

342 *Enthalpy of hydrate dissociation (ΔH_{diss}) for CH_4 mixed gas hydrates in the presence*
 343 *of AILs*

344 The ΔH_{diss} values for all studied systems are presented in Table 7 and Table 8. It is
 345 already well recognized that both pure CH_4 and CO_2 form structure I hydrate
 346 [8,74,75]. Therefore, their CH_4 riched binary mixtures are likewise only formed
 347 structure I hydrates as reported in prior studies [1,19] as well. The participation of
 348 AILs in the hydrated crystalline structure identified via changes observed in the
 349 obtained ΔH_{diss} . As earlier discussed by Sloan and Koh [1] that the enthalpy of
 350 hydrate dissociation is predominantly affected by the cage occupancy of guest
 351 molecule. Thus, as the ΔH_{diss} of studied AILs are not altered in the presence of all
 352 AILs except TBAOH, it could be established that AILs are not contributing to the
 353 hydrate crystalline structure. However, in case of TBAOH ΔH_{diss} is noticeable
 354 changes in-comparisons with pure water which is attributed owing to the semi-
 355 clathratic nature of TBAOH as reported by the previous studies [70,71]. This
 356 enlightened the contribution of TBAOH molecules in the formation of hydrate cages
 357 to form semi-clathrate hydrates due to the presence of TBA^+ cation as
 358 comprehensively define by Shimada and co-workers prior [76]. Moreover, as the
 359 ΔH_{diss} is in the range of sI hydrate, it could be concluded that apart from TBAOH,
 360 only sI hydrates are formed during these experiments.

361 **Table 7:** Calculated molar enthalpies ΔH_{diss} (kJ/mol) of hydrate dissociation in the
 362 presence and absence of 10wt% aqueous AILs solution for CH_4 rich mixed gas
 363 hydrates at various equilibrium pressures

Pressure (MPa)	10 wt% aqueous AILs solutions				
	Water	TMAOH	TEAOH	TPrAOH	TBAOH
3.0	64.50	65.56	65.82	65.01	75.88
4.50	61.26	61.96	61.02	61.52	72.14

6.0	58.09	58.72	56.31	58.39	67.67
7.50	55.37	55.93	52.03	55.57	63.28
Average ΔH_{diss}	59.80	60.54	58.80	60.12	69.74

364 Expanded uncertainties U(T) = ± 0.1 K, U(P) = ± 0.01 MPa, U(mass fraction) = ± 0.0001 g, U(H) = ± 1.2 kJ·mol⁻¹ (0.95 level of
365 confidence).

366 **Table 8:** Calculated molar enthalpies ΔH_{diss} (kJ/mol) of TMAOH at different
367 concentrations (1, 5 and 10wt %) for CH₄ rich mixed gas hydrates at various
368 equilibrium pressures

Pressure (MPa)	TMAOH composition			
	0 wt%	1 wt%	5 wt%	10 wt%
3.00	64.50	65.23	65.42	65.56
4.50	61.26	61.87	62.01	61.96
6.00	58.09	58.64	58.79	58.72
7.50	55.37	55.83	56.02	55.93
Average ΔH_{diss}	59.80	60.39	60.56	60.54

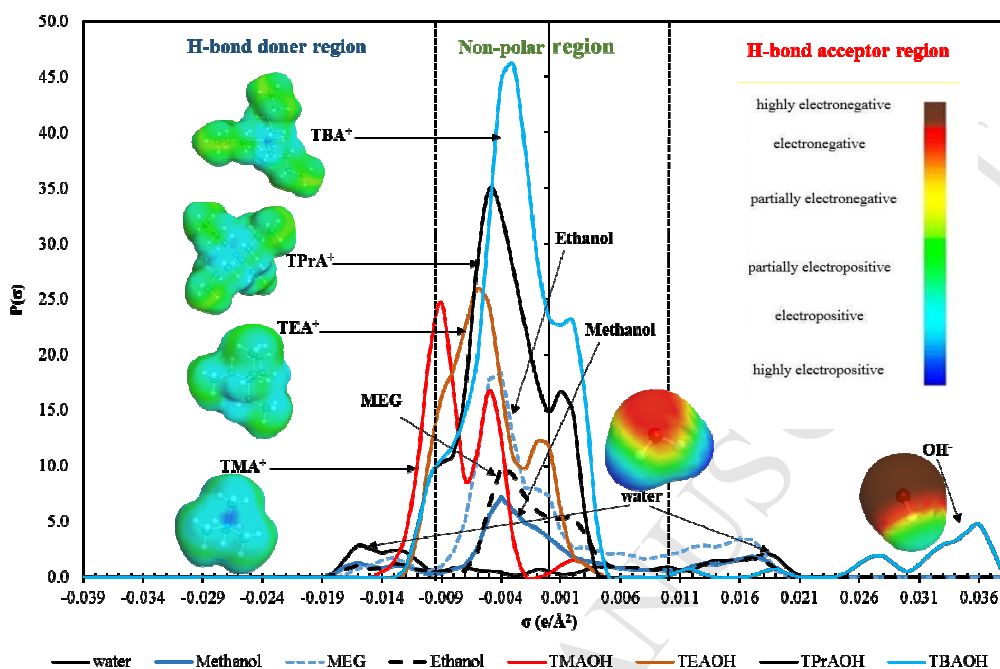
369 Expanded uncertainties U(T) = ± 0.1 K, U(P) = ± 0.01 MPa, U(mass fraction) = ± 0.0001 g, U(H) = ± 1.2 kJ·mol⁻¹ (0.95 level of
370 confidence).

371 *COSMO-RS Analysis of AILs-Water System*

372 Commonly, the chemicals which can form efficient hydrogen bonding with water
373 are apparently better thermodynamic inhibitors. The main idea to apply COSMO-RS
374 in this study to acquire the sigma profile data of the studied systems (AILs-water).
375 The sigma profile data are generated to facilitate the better understanding of the alkyl
376 chain elongation impact on the hydrophilicity and hydrogen bonding interaction of
377 studied AILs as illustrated in Figure 6. Moreover, the sigma profiles of commercial
378 THI inhibitors, i.e., methanol, MEG and ethanol are also added in Figure 6 to
379 understand the THI behaviour. According to Klamt [43], the Sigma profile can divide
380 into three (3) interaction regions. The first region at the left side outlines the most
381 electropositive area (i.e. H-bond donor). Whereas nonpolar area is the lies in the
382 middle (between -1.0 e/nm² and 1.0 e/nm²) and the right side represents highly
383 electronegative, i.e. act as H-bond acceptor region [42,62,66,77] as shown in Figure
384 6.

385 It is observed from sigma profile results in **Error! Reference source not found.6**
386 that water possessed extraordinary H-bonding donor and acceptor affinity in both
387 polar regions; this tendency ascends due to the presence of lone pairs of the oxygen
388 besides the two hydrogen atoms in its structure. Sigma profiles of conventional

389 inhibitors revealed that they possess extended and similar sigma profile peaks length
 390 like water (mainly methanol) which can efficiently interact with water with dominant
 391 hydrogen-bond exchange which ensued in higher miscibility.



392

393 **Figure 6:** COSMO-RS generated sigma profiles and sigma surfaces of studied AILs,
 394 conventional inhibitors and water systems.

395 In case of AILs, the AILs are having difference in the peak height in the same regions
 396 provide better miscibility with each other, increase in peak difference results towards
 397 lesser miscibility among them. The AILs cation having shortest alkyl chain, i.e.
 398 TMA⁺ shows the highest H-bond donor ability due to engaging some area in the H-
 399 bond donor region together with lowest peak difference (21.818) among water in
 400 nonpolar regions. On the contrary, The OH⁻ anion shows a peak on the extreme right
 401 side of Figure 5 which indicated its powerful H-bond acceptor ability. Another
 402 essential reason makes OH⁻ more suitable anion is there lowest peak difference
 403 (2.931) in H-bond acceptor region with a water molecule. The minor difference
 404 among peaks together higher H-bond acceptor affinity results in the form of
 405 potentially better hydrate inhibition performance. Moreover, the presence of TMA⁺
 406 cation rises the hydrophilicity of TMAOH consequent in higher thermodynamic
 407 inhibition impact compared to the other studied AILs. Furthermore, TMAOH
 408 possesses TMA⁺ cation which contains only one alkyl group (methyl) which also
 409 offer sufficient linkage at the surface of gas and water interface, display
 410 comparatively hydrophilic behaviour compared to higher alkyl chain AILs [25,29].

411 The peak difference further extended as the alkyl chain length of the AILs increases
412 as in the case of TEOH, TPrAOH and TBAOH [12]. Interestingly, the trend of
413 sigma profile data analysis further justified the THI inhibition behaviour of
414 considered AILs.

415 Preceding Literature [14,25] has previously recognized that the THI behaviour is
416 favourably reliant on the hydrogen bonding ability of anion like OH⁻ together with the
417 elongation of cations alkyl chain length as confirmed via sigma profile analysis (see
418 Figure 5. Apparent thermodynamic inhibition of AILs is very sensitive to the change
419 in cation, primarily due to microscopic level hydrogen bonding interactions of
420 between AILs and water molecules [78]. The hydrogen bonds and electrostatic
421 interactions of AILs considerably lower the activity coefficient of water, and therefore
422 lead to robust THI inhibition [79]. Thus the better hydrate inhibition performance of
423 TMAOH (as witnessed in Figure 3, and Figure 3, $\Delta T_f = 1.28$ K) is due to the presence
424 of shortest alkyl chain cation (methyl -CH₃) [TMA⁺] among all the studied system as
425 confirmed by the Figure 5. Additionally, Kurnia *et al.*[80], stated the increase in the
426 size of alkyl chain length increase the aliphatic-moieties associated with the cation
427 core of AILs leads towards the hydrophobicity of AILs and hence to decline the AILs
428 mutual miscibility with water which attributed due to the influence of cations in the
429 considered AILs. Moreover, the presence of OH⁻ functional group, significantly
430 increases the nonideality of the system by altering the chemical potential as revealed
431 by elsewhere [21]. Nevertheless, both conventional inhibitors and AILs show peaks in
432 all the sigma profile regions like water. However, COSMO-RS data further
433 corroborated the superior THI impact of conventional over studied AILs.

434 *Thermodynamic modelling of CH₄ riched mixed gas hydrate in the presence of AILs*

435 The considered electrolyte model (Dickens and Quinby-Hunt [50] model) is
436 utilize to predict the HL_w/VE data for studied systems with AILs solutions. Since the
437 considered model use freezing point (T_f) depression temperatures of the electrolyte,
438 the T_f of the studied AILs solutions are calculated as proposed by Dickens and
439 Quinby-Hunt [50] and reported in Table 9.

$$435 \quad T_f = -k_f(m)(i) \quad (8)$$

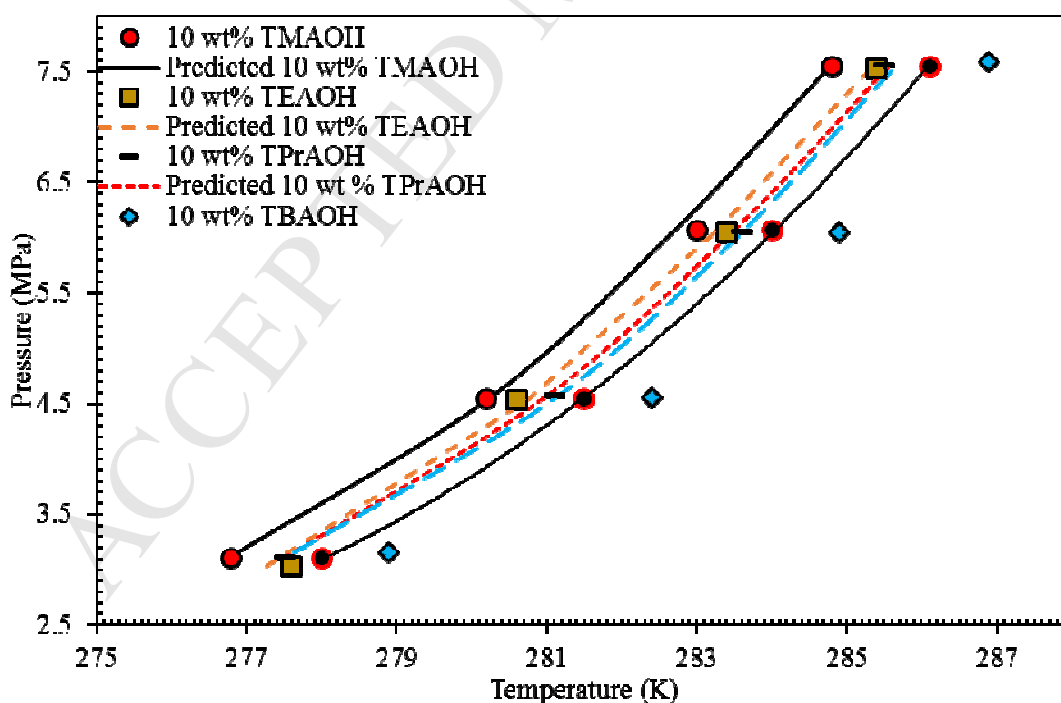
440 where, k_f represents the cryoscopic constant of water as 1.853 K·kg/mol, m denoted
441 the molality of the AILs, and i represents the ionic strength of the AILs.

442 **Table 9:** The calculated freezing point temperatures T_f (K) of studied AILs solutions.

AILs concentrations	TMAOH	TEAOH	TPrAOH	TBAOH
1 wt%	272.77 K	-	-	-
5 wt%	271.87 K	-	-	-
10 wt%	270.73 K	271.60 K	271.99 K	272.20 K

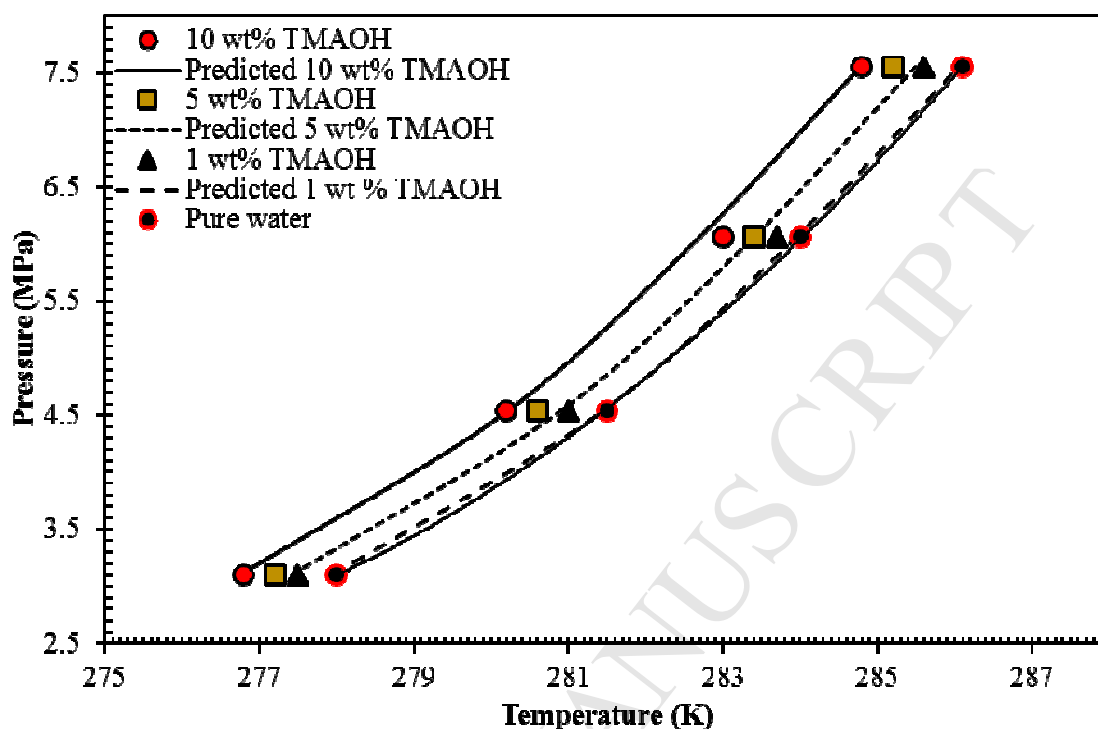
443 Expanded uncertainties $U(T) = \pm 0.1$ K, (0.95 level of confidence).

444 As is observed from Table 9 that the freezing point of the AILs systems increased
 445 with the elongation of the alkyl chain. As a result, TMAOH offers the lowermost
 446 freezing point which endorsed in the form of superior THI inhibition. The predicted
 447 and experimental HL_w VE data points for 10 wt% aqueous AILs solutions depicted in
 448 Figure 6. Furthermore, the modelling is extended to the various concentrations of
 449 TMAOH solution and presented in Figure 7.



450

451 **Figure 7:** Experimental and predicted HL_w VE data points for 10 wt% AILs systems
 452 with CH_4 riched mixed gas.



453

454 **Figure 8:** Experimental and predicted HL_wVE data for 1, 5 and 10 wt% TMAOH with
 455 CH_4 riched mixed gas.

456 As demonstrated in the above figures, the predicted HL_wVE modelling results are in
 457 satisfactory agreement with experimental data. Table 10 further presented the average
 458 absolute error for prediction of CH_4 rich mixed gas HL_wVE points of studied systems.
 459 Also, robust correlations with R^2 values < 0.99 at 95 % confidence level attained
 460 among the experimental and predicted HL_wVE data in the presence of shorter alkyl
 461 chain AILs (TMAOH, TEAOH and TPrAOH). Owing to semi-clathratic nature of
 462 TBAOH, the existing model is not capable of pertinent the TBAOH behaviour. As
 463 stated earlier, the considered electrolyte model established upon the freezing point
 464 depression temperatures of the AILs. Ideally, TBAOH supposes to provide slight
 465 inhibition at 10wt% concentration instead it delivers hydrate promotional impact
 466 attributed due to its semi-clathratic nature caused in overprediction as evident in AAE
 467 value of 1.28 K (see Table 10). The enthalpy of TBAOH data in this study also
 468 confirmed the semi-clathratic nature of TBAOH which previously reported for
 469 different gases systems [26,70,81,82]. It can also conclude from TBAOH result that

470 the existing model is not appropriate for semi-clathrate hydrates. Moreover, the
 471 accuracy of the model at low concentration (i.e. 1wt% TMAOH) is found least precise
 472 than other concentrations perhaps owing to a smaller extent of freezing point
 473 depression at 1 wt% aqueous TMAOH solution. Overall, this can be concluded that,
 474 in hydrate formation conditions, aqueous AILs have the same behaviour as
 475 electrolytes. Therefore, the existing model could employed efficiently or modified for
 476 the modelling of the HL_w VE conditions in the presence of different ionic liquids for
 477 other hydrate formers.

478 **Table 10:** Predicted HL_w VE points in the presence of studied AILs systems.

System	Temperature range (K)	No. data point	AAE (K)	R ²
10 wt% aqueous AILs solutions				
TMAOH	276.7-284.7	4	0.10	0.998
TEAOH	277.2-285.3	4	0.18	0.997
TPrAOH	277.5-285.5	4	0.08	0.999
TBAOH	277.6-285.7	4	1.26	0.999
TMAOH solutions				
1 wt%	278.0-286.1	4	0.40	0.999
5 wt%	277.4-285.5	4	0.20	0.998
10 wt%	276.7-284.7	4	0.10	0.998

479 CONCLUSION

480 In this study, the HL_w VE behaviour of CH₄ rich binary mixed gas in the presence of
 481 four AILs are reported via experimental and modelling approaches. Results indicated
 482 that in the presence of shorter alkyl chain AILs (TMAOH, TEAOH and TPrAOH at
 483 10wt % concentration) the hydrate phase boundary CH₄ riched gas moves to higher
 484 pressure and lower temperature regions. Conversely, TBAOH displayed hydrate
 485 promotional influence in this study. The average suppression temperature (ΔT)
 486 between 10wt% AILs systems ranged between 1.28 K (TMAOH) to -0.84 K
 487 (TBAOH) within the studied pressure range (1.90-5.10 MPa). It is apparent from the

488 accomplished results that the THI inhibition profoundly linked to the alkyl chain
489 length of cation (elongation) of AILs. Thus, shorter alkyl chain delivers enhanced
490 thermodynamic inhibition in comparison to higher alkyl chain length AILs. The THI
491 impact of TMAOH (best found AIL in this study) also extended to various
492 concentrations (1, 5 and 10 wt %) and found that THI inhibition reduced with
493 decreased concentrations of TMAOH. Sigma profile data of considered AILs from
494 COSMO-RS provide additional justification on the influence of alkyl chain length
495 (elongation) of AILs on THI inhibition. Moreover, the dissociation enthalpy of CH₄
496 riched mixed gas (CH₄ + CO₂ + AILs-water) also reported for all the studied systems.
497 Apart from TBAOH (semi-clathrate), the enthalpy data of all other (considered) AILs
498 are in the range of the structure I hydrate. Apparently; this also endorses that shorter
499 alkyl chain AILs do not partake in the hydrate cage structures. Furthermore, the
500 electrolyte based thermodynamic model applied to predict the HL_wVE data of CH₄
501 riched mixed gas hydrates in the presence of studied AILs; except for TBAOH, all the
502 considered AILs exhibited a good agreement with experimental data.

503 **Acknowledgement**

504 PETRONAS Research Sdn Bhd (PRSB) supported this study under TD Project
505 (MRA) Grant No. 053C1-024. The authors would like to recognized Chemical
506 Engineering Department, Universiti Teknologi PETRONAS for providing facilities
507 throughout the studies.

508 **References**

- 509 [1] E.D. Sloan, C.A. Koh, Clathrate Hydrates of Natural Gases, 3rd edition, CRC
510 Press Taylor & Francis, Boca Raton; London; New York, 2008.
- 511 [2] C.E. Taylor, J.T. Kwan, eds., Advances In the Study of Gas Hydrates, 1st ed.,
512 Kluwer Academic Publishers New York, Boston, Dordrecht, London, Moscow,
513 2004.
- 514 [3] M.L. Zanota, C. Dicharry, A. Graciaa, Hydrate plug prevention by quaternary
515 ammonium salts, Energy and Fuels. 19 (2005) 584–590.
516 doi:10.1021/ef040064l.
- 517 [4] M.S. Khan, C.B. Bavoh, B. Partoon, B. Lal, M.A. Bustam, A.M. Shariff,
518 Thermodynamic effect of ammonium based ionic liquids on CO₂ hydrates
519 phase boundary, J. Mol. Liq. 238 (2017) 533–539.
520 doi:10.1016/j.molliq.2017.05.045.

- 521 [5] Z.D. Patel, J. Russum, Flow Assurance: Chemical inhibition of gas hydrates in
522 deepwater production systems, *Multi-Chem.* (2009) 4. doi:10.4043/14010-MS.
- 523 [6] L.K. Chun, A. Jaafar, Ionic liquid as low dosage hydrate inhibitor for flow
524 assurance in pipeline, *Asian J. Sci. Res.* 6 (2013) 374–380.
525 doi:10.3923/ajsr.2013.374.380.
- 526 [7] D. Sloan, C. Koh, A. Sum, *Natural gas hydrates in flow assurance*, Gulf
527 Professional Publishing, 2010.
- 528 [8] Q. Nasir, K.K. Lau, B. Lal, K.M. Sabil, Hydrate Dissociation Condition
529 Measurement of CO₂ - Rich Mixed Gas in the Presence of Methanol / Ethylene
530 Glycol and Mixed Methanol / Ethylene Glycol + Electrolyte Aqueous Solution,
531 *J. Chem. Eng. Data.* 59 (2014) 3920–3926.
- 532 [9] A.K. Sum, C.A. Koh, E.D. Sloan, Clathrate Hydrates: From Laboratory
533 Science to Engineering Practice, *Ind. Eng. Chem. Res.* 48 (2009) 7457–7465.
534 doi:10.1021/ie900679m.
- 535 [10] M. Cha, K. Shin, Y. Seo, J.Y. Shin, S.P. Kang, Catastrophic growth of gas
536 hydrates in the presence of kinetic hydrate inhibitors, *J. Phys. Chem. A.* 117
537 (2013) 13988–13995. doi:10.1021/jp408346z.
- 538 [11] C. Xiao, H. Adidharma, Dual function inhibitors for methane hydrate, *Chem.*
539 *Eng. Sci.* 64 (2009) 1522–1527. doi:10.1016/j.ces.2008.12.031.
- 540 [12] X. Peng, Y. Hu, Y. Liu, C. Jin, H. Lin, Separation of ionic liquids from dilute
541 aqueous solutions using the method based on CO₂ hydrates, *J. Nat. Gas Chem.*
542 19 (2010) 81–85. doi:10.1016/S1003-9953(09)60027-X.
- 543 [13] K.M. Sabil, O. Nashed, B. Lal, L. Ismail, A. Japper-Jaafar, A. Japper-, et al.,
544 Experimental investigation on the dissociation conditions of methane hydrate
545 in the presence of imidazolium-based ionic liquids, *J. Chem. Thermodyn.* 84
546 (2015) 7–13. doi:10.1016/j.jct.2014.12.017.
- 547 [14] M. Tariq, D. Rooney, E. Othman, S. Aparicio, M. Atilhan, M. Khraisheh, Gas
548 hydrate inhibition: A review of the role of ionic liquids, *Ind. Eng. Chem. Res.*
549 53 (2014) 17855–17868. doi:10.1021/ie503559k.
- 550 [15] O. Nashed, K.M. Sabil, B. Lal, L. Ismail, A.J. Jaafar, Study of 1-(2-
551 Hydroxyethyl) 3-methylimidazolium Halide as Thermodynamic Inhibitors,
552 *Appl. Mech. Mater.* 625 (2014) 337–340.
553 doi:10.4028/www.scientific.net/AMM.625.337.
- 554 [16] V.R. Avula, R.L. Gardas, J.S. Sangwai, Modeling of Methane Hydrate
555 Inhibition in the Presence of Green Solvent for Offshore Oil and Gas Pipeline,
556 *Isope-I-14.* 3 (2014) 49–54.
- 557 [17] T.E. Rufford, S. Smart, G.C.Y. Watson, B.F. Graham, J. Boxall, J.C. Diniz da
558 Costa, et al., The removal of CO₂ and N₂ from natural gas: A review of
559 conventional and emerging process technologies, *J. Pet. Sci. Eng.* 94–95 (2012)
560 123–154. doi:10.1016/j.petrol.2012.06.016.
- 561 [18] K. Nazari, A.N. Ahmadi, A Thermodynamic Study Of Methane Hydrate
562 Formation In The Presence Of [BMIM][BF₄] and [BMIM][Ms] Ionic Liquids,
563 in: *Proc. 7th Int. Conf. Gas Hydrates (ICGH 2011)*, 2011.
- 564 [19] O. Nashed, D. Dadebayev, M.S. Khan, C.B. Bavoh, B. Lal, A.M. Shariff,
565 Experimental and modelling studies on thermodynamic methane hydrate

- 566 inhibition in the presence of ionic liquids, *J. Mol. Liq.* 249 (2018) 886–891.
567 doi:10.1016/j.molliq.2017.11.115.
- 568 [20] J.H. Cha, C. Ha, S.P. Kang, J.W. Kang, K.S. Kim, Thermodynamic inhibition
569 of CO₂ hydrate in the presence of morpholinium and piperidinium ionic
570 liquids, *Fluid Phase Equilib.* 413 (2016) 75–79.
571 doi:10.1016/j.fluid.2015.09.008.
- 572 [21] L. Keshavarz, J. Javanmardi, A. Eslamimanesh, A.H. Mohammadi,
573 Experimental measurement and thermodynamic modeling of methane hydrate
574 dissociation conditions in the presence of aqueous solution of ionic liquid,
575 *Fluid Phase Equilib.* 354 (2013) 312–318. doi:10.1016/j.fluid.2013.05.007.
- 576 [22] X. Shen, L. Shi, Z. Long, X. Zhou, D. Liang, Experimental study on the kinetic
577 effect of N-butyl-N-methylpyrrolidinium bromide on CO₂ hydrate, *J. Mol. Liq.*
578 223 (2016) 672–677. doi:10.1016/j.molliq.2016.08.111.
- 579 [23] K.-S. Kim, J.W. Kang, S.-P. Kang, Tuning ionic liquids for hydrate inhibition,
580 *Chem. Commun.* 47 (2011) 6341–6343. doi:10.1039/c0cc05676f.
- 581 [24] M.S. Khan, B. Lal, B. Partoon, L.K. Keong, M.A. Bustam, N.B. Mellon,
582 Experimental Evaluation of a Novel Thermodynamic Inhibitor for CH₄ and
583 CO₂ Hydrates, *Procedia Eng.* 148 (2016) 932–940.
584 doi:10.1016/j.proeng.2016.06.433.
- 585 [25] M.S. Khan, B. Lal, C.B. Bavoh, L.K. Keong, A. Bustam, Influence of
586 Ammonium based Compounds for Gas Hydrate Mitigation : A Short Review,
587 *Indian J. Sci. Technol.* 10 (2017) 1–6. doi:10.17485/ijst/2017/v10i5/99734.
- 588 [26] O. Nashed, J.C.H. Koh, B. Lal, Physical-chemical Properties of Aqueous
589 TBAOH Solution for Gas Hydrates Promotion, *Procedia Eng.* 148 (2016)
590 1351–1356. doi:10.1016/j.proeng.2016.06.586.
- 591 [27] A. ESLAMIMANESH, Thermodynamic Studies on Semi-Clathrate Hydrates
592 of TBAB + Gases Containing Carbon Dioxide, 2012.
- 593 [28] B.S. Shin, E.S. Kim, S.K. Kwak, J.S. Lim, K.S. Kim, J.W. Kang,
594 Thermodynamic inhibition effects of ionic liquids on the formation of
595 condensed carbon dioxide hydrate, *Fluid Phase Equilib.* 382 (2014) 270–278.
596 doi:10.1016/j.fluid.2014.09.019.
- 597 [29] M.S. Khan, B. Partoon, C.B. Bavoh, B. Lal, N.B. Mellon, Influence of
598 tetramethylammonium hydroxide on methane and carbon dioxide gas hydrate
599 phase equilibrium conditions, *Fluid Phase Equilib.* Volume 440 (2017) 1–8.
600 doi:10.1016/j.fluid.2017.02.011.
- 601 [30] M. Tariq, E. Connor, J. Thompson, M. Khraisheh, M. Atilhan, D. Rooney,
602 Doubly dual nature of ammonium-based ionic liquids for methane hydrates
603 probed by rocking-rig assembly, *RSC Adv.* 6 (2016) 23827–23836.
604 doi:10.1039/C6RA00170J.
- 605 [31] C.B. Bavoh, B. Partoon, B. Lal, L. Kok Keong, Methane hydrate-liquid-
606 vapour-equilibrium phase condition measurements in the presence of natural
607 amino acids, *J. Nat. Gas Sci. Eng.* 37 (2017) 425–434.
608 doi:10.1016/j.jngse.2016.11.061.
- 609 [32] C.B. Bavoh, B. Partoon, B. Lal, G. Gonfa, S. Foo Khor, A.M. Sharif, Inhibition
610 Effect of Amino Acids on Carbon Dioxide Hydrate, *Chem. Eng. Sci.* (2017).

- 611 doi:10.1016/j.ces.2017.05.046.
- 612 [33] Z. Long, X. Zhou, X. Shen, D. Li, D. Liang, Phase Equilibria and Dissociation
613 Enthalpies of Methane Hydrate in Imidazolium Ionic Liquid Aqueous
614 Solutions, *Ind. Eng. Chem. Res.* 54 (2015) 11701–11708.
615 doi:10.1021/acs.iecr.5b03480.
- 616 [34] M.J. Ross, L.S. Toczylkin, Hydrate dissociation pressures for methane or
617 ethane in the presence of aqueous solutions of triethylene glycol, *J. Chem. Eng.*
618 *Data.* 37 (1992) 488–491. doi:10.1021/jc00008a026.
- 619 [35] A.H. Mohammadi, D. Richon, Phase Equilibria of Methane Hydrates in the
620 Presence of Methanol and/or Ethylene Glycol Aqueous Solutions, *Ind. Eng.*
621 *Chem. Res.* 49 (2010) 925–928. doi:10.1021/ie901357m.
- 622 [36] D.B.R. Heng-Joo Ng, H.J. Ng, D.B. Robinson, Hydrate formation in systems
623 containing methane, ethane, propane, carbon dioxide or hydrogen sulfide in the
624 presence of methanol, *Fluid Phase Equilib.* 21 (1985) 145–155.
625 doi:10.1016/0378-3812(85)90065-2.
- 626 [37] E. Breland, P. Englezos, Equilibrium hydrate formation data for carbon dioxide
627 in aqueous glycerol solutions, *J. Chem. Eng. Data.* 41 (1996) 11–13.
628 doi:10.1021/jc950181y.
- 629 [38] J.-H. Cha, C. Ha, S.-P. Kang, J.W. Kang, K.-S. Kim, Thermodynamic
630 inhibition of CO₂ hydrate in the presence of morpholinium and piperidinium
631 ionic liquids, *Fluid Phase Equilib.* (2015) 2–6. doi:10.1016/j.fluid.2015.09.008.
- 632 [39] X.-D. Shen, Z. Long, L. Shi, D.-Q. Liang, Phase Equilibria of CO₂ Hydrate in
633 the Aqueous Solutions of *N*-Butyl-*N*-methylpyrrolidinium Bromide, *J. Chem.*
634 *Eng. Data.* 60 (2015) 3392–3396. doi:10.1021/acs.jced.5b00652.
- 635 [40] R. Ullah, M. Atilhan, B. Anaya, M. Khraisheh, G. García, A. ElKhattat, et al.,
636 A detailed study of cholinium chloride and levulinic acid deep eutectic solvent
637 system for CO₂ capture via experimental and molecular simulation approaches,
638 *Phys. Chem. Chem. Phys.* 17 (2015) 20941–20960. doi:10.1039/C5CP03364K.
- 639 [41] M.F. Qureshi, M. Atilhan, T. Altamash, M. Tariq, M. Khraisheh, S. Aparicio,
640 et al., Gas Hydrate Prevention and Flow Assurance by Using Mixtures of Ionic
641 Liquids and Synergent Compounds: Combined Kinetics and Thermodynamic
642 Approach, *Energy & Fuels.* 30 (2016) 3541–3548.
643 doi:10.1021/acs.energyfuels.5b03001.
- 644 [42] C.B. Bavoh, B. Lal, O. Nashed, M.S. Khan, K.K. Lau, M.A. Bustam, COSMO-
645 RS: An ionic liquid prescreening tool for gas hydrate mitigation, *Chinese J.*
646 *Chem. Eng.* 24 (2016) 1619–1624. doi:10.1016/j.cjche.2016.07.014.
- 647 [43] A. Klamt, COSMO-RS for aqueous solvation and interfaces, *Fluid Phase*
648 *Equilib.* 407 (2016) 152–158. doi:10.1016/j.fluid.2015.05.027.
- 649 [44] M.S. Khan, C.S. Liew, K.A. Kurnia, B. Cornelius, B. Lal, Application of
650 COSMO-RS in Investigating Ionic Liquid as Thermodynamic Hydrate
651 Inhibitor for Methane Hydrate, *Procedia Eng.* 148 (2016) 862–869.
652 doi:10.1016/j.proeng.2016.06.452.
- 653 [45] V.R. Avula, R.L. Gardas, J.S. Sangwai, An improved model for the phase
654 equilibrium of methane hydrate inhibition in the presence of ionic liquids, *Fluid*
655 *Phase Equilib.* 382 (2014) 187–196. doi:10.1016/j.fluid.2014.09.005.

- 656 [46] V.R. Avula, R.L. Gardas, J.S. Sangwai, An efficient model for the prediction of
657 CO₂ hydrate phase stability conditions in the presence of inhibitors and their
658 mixtures, *J. Chem. Thermodyn.* 85 (2015) 163–170.
659 doi:10.1016/j.jct.2015.01.009.
- 660 [47] J. Palomar, J.S. Torrecilla, J. Lemus, V.R. Ferro, F. Rodriguez, Prediction of
661 non-ideal behavior of polarity/polarizability scales of solvent mixtures by
662 integration of a novel COSMO-RS molecular descriptor and neural networks,
663 *Phys Chem Chem Phys.* 10 (2008) 5967–5975. doi:10.1039/b807617k.
- 664 [48] B. Partoon, N.M.S. Wong, K.M. Sabil, K. Nasrifar, M.R. Ahmad, A study on
665 thermodynamics effect of [EMIM]-Cl and [OH-C₂MIM]-Cl on methane
666 hydrate equilibrium line, *Fluid Phase Equilib.* 337 (2013) 26–31.
- 667 [49] H.Y. Chin, B.S. Lee, Y.P. Chen, P.C. Chen, S.T. Lin, L.J. Chen, Prediction of
668 phase equilibrium of methane hydrates in the presence of ionic liquids, *Ind.*
669 *Eng. Chem. Res.* 52 (2013) 16985–16992. doi:10.1021/ie4027023.
- 670 [50] G.R. Dickens, M.S. Quinby-Hunt, Methane hydrate stability in pore water: A
671 simple theoretical approach for geophysical applications, *J. Geophys. Res.* 102
672 (1997) 773–783. doi:10.1029/96jb02941.
- 673 [51] M.S. Khan, C.B. Bavoh, B. Partoon, O. Nashed, B. Lal, N.B. Mellon, Impacts
674 of ammonium based ionic liquids alkyl chain on thermodynamic hydrate
675 inhibition for carbon dioxide rich binary gas, *J. Mol. Liq.* 261 (2018) 283–290.
676 doi:10.1016/j.molliq.2018.04.015.
- 677 [52] C.B. Bavoh, O. Nashed, M. Saad Khan, B. Partoon, B. Lal, A.M. Sharif, The
678 Impact of Amino Acids on Methane Hydrate Phase Boundary and Formation
679 kinetics, *J. Chem. Thermodyn.* 117 (2018) 48–53.
680 doi:10.1016/j.jct.2017.09.001.
- 681 [53] B. Partoon, K.M. Sabil, H. Roslan, B. Lal, L.K. Keong, Impact of acetone on
682 phase boundary of methane and carbon dioxide mixed hydrates, *Fluid Phase*
683 *Equilib.* 412 (2016) 51–56. doi:10.1016/j.fluid.2015.12.027.
- 684 [54] M.S. Khan, C.B. Bavoh, B. Partoon, O. Nashed, B. Lal, N.B. Mellon, Impacts
685 of ammonium based ionic liquids alkyl chain on thermodynamic hydrate
686 inhibition for carbon dioxide rich binary gas, *J. Mol. Liq.* (2018).
687 doi:10.1016/j.molliq.2018.04.015.
- 688 [55] C. Xiao, N. Wibisono, H. Adidharma, Dialkylimidazolium halide ionic liquids
689 as dual function inhibitors for methane hydrate, *Chem. Eng. Sci.* 65 (2010)
690 3080–3087. doi:10.1016/j.ces.2010.01.033.
- 691 [56] P. Babu, P. Paricaud, P. Linga, Experimental measurements and modeling of
692 the dissociation conditions of semiclathrate hydrates of tetrabutyl ammonium
693 nitrate and carbon dioxide, *Fluid Phase Equilib.* 413 (2016) 80–85.
694 doi:10.1016/j.fluid.2015.08.034.
- 695 [57] P. Babu, P. Linga, R. Kumar, P. Englezos, A review of the hydrate based gas
696 separation (HBGS) process for carbon dioxide pre-combustion capture, *Energy.*
697 85 (2015) 261–279. doi:10.1016/j.energy.2015.03.103.
- 698 [58] G.K. Anderson, Enthalpy of dissociation and hydration number of methane
699 hydrate from the Clapeyron equation, *J. Chem. Thermodyn.* 36 (2004) 1119–
700 1127. doi:10.1016/j.jct.2004.07.005.

- 701 [59] W. Lin, a. Delahaye, L. Fournaison, Phase equilibrium and dissociation
702 enthalpy for semi-clathrate hydrate of CO₂ + TBAB, *Fluid Phase Equilib.* 264
703 (2008) 220–227. doi:10.1016/j.fluid.2007.11.020.
- 704 [60] K. Tumba, P. Reddy, P. Naidoo, D. Ramjugernath, A. Eslamimanesh, A.H.
705 Mohammadi, et al., Phase equilibria of methane and carbon dioxide clathrate
706 hydrates in the presence of aqueous solutions of tributylmethylphosphonium
707 methylsulfate ionic liquid, *J. Chem. Eng. Data.* 56 (2011) 3620–3629.
708 doi:10.1021/je200462q.
- 709 [61] L. li Shi, D. qing Liang, Thermodynamic model of phase equilibria of
710 tetrabutyl ammonium halide (fluoride, chloride, or bromide) plus methane or
711 carbon dioxide semiclathrate hydrates, *Fluid Phase Equilib.* 386 (2015) 149–
712 154. doi:10.1016/j.fluid.2014.12.004.
- 713 [62] A. Klamt, F. Eckert, W. Arlt, COSMO-RS - An Alternative to Simulation for
714 Calculating Thermodynamic Properties of Liquid Mixtures, *Annu. Rev. Chem.*
715 *Biomol. Eng.* 1 (2010) 101–122. doi:10.1146/annurev-chembioeng-073009-
716 100903.
- 717 [63] A. Klamt, F. Eckert, COSMO-RS: A novel and efficient method for the a priori
718 prediction of thermophysical data of liquids, *Fluid Phase Equilib.* 172 (2000)
719 43–72. doi:10.1016/S0378-3812(00)00357-5.
- 720 [64] A. Klamt, The COSMO and COSMO-RS solvation models, *Wiley Interdiscip.*
721 *Rev. Comput. Mol. Sci.* 1 (2011) 699–709. doi:10.1002/wcms.56.
- 722 [65] C. Loschen, A. Klamt, Prediction of solubilities and partition coefficients in
723 polymers using COSMO-RS, *Ind. Eng. Chem. Res.* 53 (2014) 11478–11487.
724 doi:10.1021/ie501669z.
- 725 [66] M. Diedenhofen, A. Klamt, COSMO-RS as a tool for property prediction of IL
726 mixtures-A review, *Fluid Phase Equilib.* 294 (2010) 31–38.
727 doi:10.1016/j.fluid.2010.02.002.
- 728 [67] A.P. Pieroen, Gas hydrates- approximate relations between heat formation,
729 composition and equilibrium temperature lowering by inhibitors, *Rec. Trav.*
730 *Chim.* 74 (1955) 955–1002.
- 731 [68] J. Javanmardi, M. Moshfeghian, R.N. Maddox, An accurate model for
732 prediction of gas hydrate formation conditions in mixtures of aqueous
733 electrolyte solutions and alcohol, *Can. J. Chem. Eng.* 79 (2001) 367–373.
- 734 [69] J. Javanmardi, M. Moshfeghian, R.N. Maddox, Simple Method for Predicting
735 Gas-Hydrate-Forming, *Energy & Fuels.* 28 (1998) 219–222.
- 736 [70] Y. Su, D.J. Searles, L. Wang, Semiclathrate hydrates of methane +
737 tetraalkylammonium hydroxides, *Fuel.* 203 (2017) 618–626.
738 doi:10.1016/j.fuel.2017.05.005.
- 739 [71] O. Dolotko, A.A. Karimi, D. Dalmazzone, The Phase Behaviours in Mixed G +
740 Tetra – N-Butylphosphonium Borohydride and G + Tetra-N-Butylammonium
741 Hydroxide Hydrates (Where G = H₂, N₂), in: *Proc. 7th Int. Conf. Gas Hydrates*
742 *(ICGH 2011)*, Edinburgh, Scotland, United Kingdom, July 17-21, 2011, 2011.
- 743 [72] F. Franks, Water, *A Comprehensive Treatise: Volume 2: Water in crystalline*
744 *hydrates; aqueous solutions of simple nonelectrolytes*, Springer
745 *Science+Business Media*, 1973. doi:10.1007/978-1-4757-6958-6_2.

- 746 [73] N.N. Nguyen, A. V. Nguyen, Hydrophobic Effect on Gas Hydrate Formation in
747 the Presence of Additives, *Energy & Fuels*. (2017) [acs.energyfuels.7b01467](https://doi.org/10.1021/acs.energyfuels.7b01467).
748 [doi:10.1021/acs.energyfuels.7b01467](https://doi.org/10.1021/acs.energyfuels.7b01467).
- 749 [74] Q. Nasir, K.M. Sabil, K.K. Lau, Measurement of isothermal (vapor+liquid)
750 equilibria, (VLE) for binary (CH₄+CO₂) from T=(240.35 to 293.15) K and
751 CO₂ rich synthetic natural gas systems from T=(248.15 to 279.15) K, *J. Nat.*
752 *Gas Sci. Eng.* 27 (2015) 158–167. [doi:10.1016/j.jngse.2015.08.045](https://doi.org/10.1016/j.jngse.2015.08.045).
- 753 [75] E. Dendy Sloan, C.A. Koh, *Gas Hydrates of Natural Gases*, third edition, CRC
754 Press LLC, 2000 Corporate Blvd., N.W., Boca Raton, FL 33431, USA Orders
755 from the USA and Canada (only) to CRC Press LLC, London; New York,
756 2008.
- 757 [76] W. Shimada, Y. Kamata, H. Oyama, T. Ebinuma, S. Takeya, T. Uchida, et al.,
758 Gas Separation Method Using Tetra-n-butyl Ammonium Bromide Semi-
759 Clathrate Hydrate, *Japanese J. Appl. Physics, Part 1 Regul. Pap. Short Notes*
760 *Rev. Pap.* 43 (2004) 362–365. [doi:10.1143/JJAP.42.L129](https://doi.org/10.1143/JJAP.42.L129).
- 761 [77] G. Gonfa, M.A. Bustam, T. Murugesan, Z. Man, M.I.A. Mutalib, COSMO-RS
762 Based Screening Ionic Liquids for Separation of Benzene and Cyclohexane,
763 *Int. J. Chem. Environ. Eng.* 3 (2012) 244–254.
- 764 [78] T. Kavitha, P. Attri, P. Venkatesu, R.S.R. Devi, T. Hofman, Influence of alkyl
765 chain length and temperature on thermophysical properties of ammonium-
766 based ionic liquids with molecular solvent, *J. Phys. Chem. B.* 116 (2012)
767 4561–4574. [doi:10.1021/jp3015386](https://doi.org/10.1021/jp3015386).
- 768 [79] J.-H. Sa, G.-H. Kwak, K. Han, D. Ahn, S.J. Cho, J.D. Lee, et al., Inhibition of
769 methane and natural gas hydrate formation by altering the structure of water
770 with amino acids, *Sci. Rep.* 6 (2016) 31582. [doi:10.1038/srep31582](https://doi.org/10.1038/srep31582).
- 771 [80] K.A. Kurnia, M. V. Quental, L.M.N.B.F. Santos, M.G. Freire, J.A.P. Coutinho,
772 Mutual solubilities between water and non-aromatic sulfonium-, ammonium-
773 and phosphonium-hydrophobic ionic liquids., *Phys. Chem. Chem. Phys.* 17
774 (2015) 4569–77. [doi:10.1039/c4cp05339g](https://doi.org/10.1039/c4cp05339g).
- 775 [81] A.A. Karimi, O. Dolotko, D. Dalmazzone, Hydrate phase equilibria data and
776 hydrogen storage capacity measurement of the system H₂+tetrabutylammonium
777 hydroxide+H₂O, *Fluid Phase Equilib.* 361 (2014) 175–180.
778 [doi:10.1016/j.fluid.2013.10.043](https://doi.org/10.1016/j.fluid.2013.10.043).
- 779 [82] Y. Su, S. Bernardi, D.J. Searles, L. Wang, Effect of Carbon Chain Length of
780 Organic Salts on the Thermodynamic Stability of Methane Hydrate, *J. Chem.*
781 *Eng. Data.* 61 (2016) 1952–1960. [doi:10.1021/acs.jced.6b00185](https://doi.org/10.1021/acs.jced.6b00185).

Research Highlights

- Elongation of AILs alkyl chain attributed decline in THI.
- Enthalpy of hydrate dissociations data reported for CH₄ riched mixed gas systems.
- COSMO-RS based sigma profile analysis justified the THI behavior of studied AILs.
- The experimental and model predicted HL_wVE data are found to be in good agreement.